Structural and hydrodynamic characteristics of polystyrene synthesized in the presence of conjugated dinitrones

E. V. Kolyakina, A. B. Alyeva, E. A. Zakharychev, and D. F. Grishin★

[a]*N. I. Lobachevsky State University of Nizhny Novgorod, 23 prosp. Gagarina, 603950 Nizhny Novgorod, Russian Federation. Phone: +7 (831) 462 3550. E-mail: grishin@ichem.unn.ru*

A series of branched high-molecular-weight alkoxyamines (HAAs) based on polystyrene of different molecular weight were synthesized using nitroxide radicals generated *in situ* in the presence of conjugated dinitrones (*N*,*N*-dimethylglyoxaldinitrone, *N*,*N*-di-*tert*-butylglyoxaldinitrone, and *N*,*N*-diphenylglyoxaldinitrone). Structural features of the products obtained were studied by MALDI-TOF mass spectrometry. Modification of the synthesized HAAs in the presence of azobisisobutyronitrile, carbon tetrabromide, dodecyl mercaptane, 4,5,5-trimethyl-2,2-diethyl-2,5-dihydroimidazole-1-oxyl, and 3,5-di-*tert*-butylbenzoquinone, as well as thermolysis of the HAAs in the presence of atmospheric oxygen showed that the nitroxide fragments are located within the polymer chain irrespective of the initial structure of the conjugated dinitrone. The molecular weight characteristics and conformational properties of the nitroxide-containing linear macromolecules and polymers were studied by static and dynamic light scattering and by viscometry. In most cases, the calculated values of the ρ-parameter (R_g/R_h) and the Zimm viscosity factor of the branched polystyrene samples synthesized using conjugated dinitrones are lower than those of linear analogues.

Key words: radical polymerization, polystyrene, nitroxide radicals, dinitrones, hydrodynamic characteristics, form factor.

The concept of controlled radical polymerization (CRP) developed in the last two decades opened new prospects in polymer chemistry.[1—4] There are three main routes in CRP, *viz.*, stable free-radical polymerization (SFRP), atom transfer radical polymerization (ATRP), and reversible addition-fragmentation chain-transfer polymerization (RAFT). They provide powerful tools for the synthesis of polymers with specified molecular weight (MW), chemical structure, and architecture including dendrimers, hyperbranched polymers, multiple-arm stars, molecular brushes, and other macromolecular structures.[1—8]

Among these CRP methods, SFRP, or the synthesis of polymers mediated by stable nitroxide radicals in the reversible inhibition regime, is one of the best studied approaches that does not require additional purification of polymers from catalysts.[9—11] Stable nitroxide radicals and alkoxyamines (AAs) used as main SFRP agents are often synthesized from commercially available spin traps. The spin trap based AAs can be obtained either *ex situ* (with preliminary synthesis and isolation of AAs)[9,10] or *in situ* (during the polymerization process).[12—22] Implementation of the latter technique in the SFRP strategy opened new prospects for the synthesis of high-molecular-weight alkoxyamines (HAAs) and (co)polymers with specified structure and topology and allowed one to carry out controlled synthesis in the practically more convenient temperature range (70—90 °C) and to extend the range of monomers that can be polymerized in the reversible inhibition regime.[12—22] This method of synthesis of HAAs in the monomer medium at relatively low temperatures, where the decomposition of HAAs is impossible, was called enhanced spin capturing polymerization (ESCP).[23—25] The HAAs obtained at higher temperatures (above 100 °C) were used to synthesize various block copolymers and to carry out post-polymerization.[23—25]

High-molecular-weight AAs based on spin traps with symmetric structure can also be obtained using radical trap-assisted atom transfer radical coupling (RTA-ATRC).[26—34] The technique involves the synthesis of a polymer with a particular structure and MW characteristics in the ATRP regime followed by coupling of high-molecular-weight radicals mediated by nitrones or nitroso compounds in the presence of a catalytic system based on transition metals.

These methods deserve particular attention from the standpoint of efficiency, versatility, and possibility to obtain macromolecules of complex structure and different topology. For instance, star-shaped, H-shaped, cyclic, dendritic, and other polymeric products were synthesized in the SFRP, ESCP, and RTA-ATRC regimes in

Published in Russian in *Izvestiya Akademii Nauk. Seriya Khimicheskaya,* No. 10, pp. 1997—2013, October, 2021.

1066-5285/21/7010-1997

the presence of functional nitrones.[9,30–35] Note that the development of new methods for the synthesis of branched polymers is to a great extent due to the difference of the physicochemical properties of these polymers from those of their linear analogues. Branched polymers possess a number of unique properties and have a wide variety of applications including biomedical ones.[36] In particular, star-shaped polymers are characterized by low viscosity, good solubility, high strength, encapsulability, and are used as carriers for drug and gene delivery, in tissue engineering and diagnostics, and for the design of antibacterial biomaterials.[37]

The aim of this work was to develop a strategy for the synthesis of branched styrene (ST) based polymers in the presence of spin traps, namely, conjugated dinitrones (DNs) bearing various substituents at nitrogen atom, and to study the structure and conformational properties of the polymers synthesized.

Results and Discussion

Earlier,[19] we established that HAAs obtained *in situ* during the polymerization of ST mediated by various mononitrones (*C*-phenyl-*N*-*tert*-butylnitrone, or PBN, and 2-(benzylideneamino)-2-methyl-1-phenylpropanol-1-*N*-oxide, or BMPO) can efficiently control the polymerization process in the reversible inhibition regime at temperatures below 90 °C. Here we tested this approach to the synthesis of HAAs using DNs of different structure (MDN, BDN, and PDN).

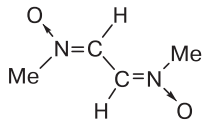

N,*N*-Dimethylglyoxaldinitrone (MDN)

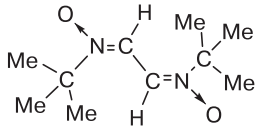

N,*N*-Di-*tert*-butylglyoxaldinitrone (BDN)

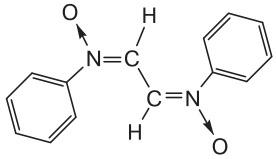

N,*N*-Diphenylglyoxaldinitrone (PDN)

It was established that these DNs efficiently control the rate of ST polymerization and the MW characteristics of polystyrene (PS) in a wide temperature range from 70 to 130 °C. For instance, in Fig. 1 the MW of PS synthesized

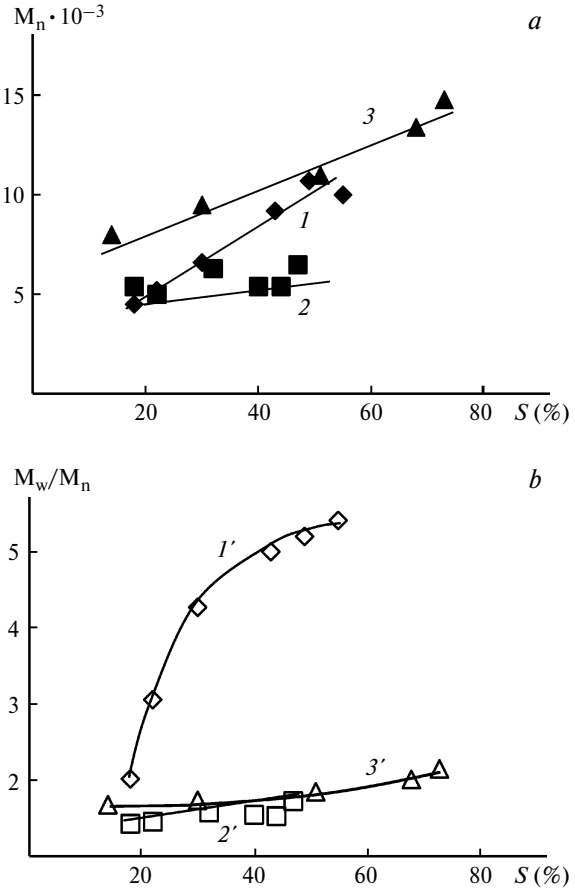

Fig. 1. Molecular weight (*a*) and dispersity (*b*) of polystyrene synthesized at 90 °C in the presence of AIBN (1 mol.%) and dinitrone (1.5 mol.%) plotted *vs.* monomer conversion: MDN (*1*, *1′*), BDN (*2*, *2′*), and PDN (3, *3′*).

in the presence of DNs (1.5 mol.%) is plotted *vs.* monomer conversion. As can be seen, the MW increases linearly with the monomer conversion in the presence of all DNs studied. However, the dispersity of PS depends strongly on the DN structure. In particular, ST polymerization in the presence of MDN affords highly disperse samples (M_w/M_n = 5.4 at 90 °C; *cf.* 2.15 for PS synthesized in the presence of PDN at deep monomer conversions). In contrast to ST polymerization in the presence of MDN and PDN, the synthesis of PS in the presence of BDN results in narrow-dispersity samples (minimum dispersity is 1.43).

Styrene polymerization mediated by glyoxal-based DNs was thoroughly studied in different temperature and concentration conditions elsewhere.[20] Note that the structure of DNs and the stability of the HAAs based on them are of great importance for implementation of the reversible inhibition regime. Indeed, steric hindrances produced by the methyl, *tert*-butyl, and phenyl substituents in the DNs are different and can immediately affect both the accepting ability of the nitrone and the lability of the

C—O bond in the HAA molecules. It is no coincidence that the HAAs based on MDN (the least sterically hindered nitrone) provide the best control of ST polymerization only at high temperatures (130 °C), as indicated by the relatively low dispersities of the PS samples synthesized in DMSO (M_w/M_n = 1.65). When using HAAs based on the other two dinitrones (BDN and PDN) bearing bulkier substituents, the optimum temperature regime of controlling the MW characteristics (70—90 °C) is similar to the conditions of industrial polymer synthesis. This allows one to obtain polymers with a dispersity of 1.42 for the BDN-mediated polymerization. At 130 °C, controlling the MW characteristics of PS in the presence of *in situ* synthesized HAAs (BDN and PDN) becomes more difficult due to the lower accepting ability of these DNs compared to MDN and to different stability of the HAAs under those conditions. In addition, the possibility to use BDN in the high-temperature regime is limited by the occurrence of side processes. In particular, BDN-based nitroxide radicals can decompose to 2-methyl-2-nitrosopropane (MNP) and *tert*-butyl vinyl nitroxides at high temperatures.[38] We also showed that an increase in the polymerization time and temperature leads to decomposition of the BDN-based HAAs, which manifests itself in changes in the color of the polymerization system to dark brown and in minor variations of the MW characteristics of PS.

Note that, unlike the mononitrones PBN and BMPO, DNs are somewhat less efficient in the *in situ* polymerization of ST aimed at obtaining narrow- dispersity polymers.[19,20] This can be due to different accepting ability of mono- and dinitrones and to the stability of the corresponding HAAs.

A distinctive feature of DNs is the possibility to mediate the synthesis of branched polymers, namely, three- and four-arm ones (Scheme 1).

Star-shaped polymers are obtained using two synthetic methodologies, a divergent (core-first) and a convergent (arm-first).[39] In this respect the *in situ* synthesis of HAAs mediated by glyoxal-based α-DNs represents an original route to branched polymers based on the divergent strategy (see Scheme 1). However, the efficiency of formation of branched HAAs can depend on the steric hindrances produced by substituents in the α-DN molecules, on the redistribution of the electron density in the initial DNs and in the products (HAAs), and on the stability of intermediates and HAAs in the course of polymerization. By and large, these factors should influence the rate constant for acceptance of chain propagation radicals by the DNs under study and, as a consequence, the ability to form star-shaped structures.

To determine the composition, structure, and conformational properties of the polymers obtained during the *in situ* synthesis of HAAs, we modified a number of polymers and analyzed their MW characteristics and structures by gel permeation chromatography (GPC), MALDI-TOF mass spectrometry as well as static and dynamic light scattering.

Modification of polystyrene synthesized in the presence of DNs and a study of its composition and structure. First, the composition of polymers synthesized by the MDN- and BDN-mediated polymerization was studied by MALDI-TOF mass spectrometry. Samples of low-molecular-weight MDN-based PS (M_n = 6000, M_w/M_n = 4.51) and BDN-based PS (M_n = 4200, M_w/M_n = 1.38) were analyzed in detail. The DN-based HAAs were analyzed using two different matrices, *trans*-2-[3-(4-*tert*-butylphenyl)-2-methyl-2-propenylidene]malonitrile (DCTB) and 2,5-dihydroxybenzoic acid (DHB) (see Figs 2 and 3, respectively). A MALDI-TOF analysis of the MDN-based HAA using the DHB and DCTB matrices revealed that the

Scheme 1

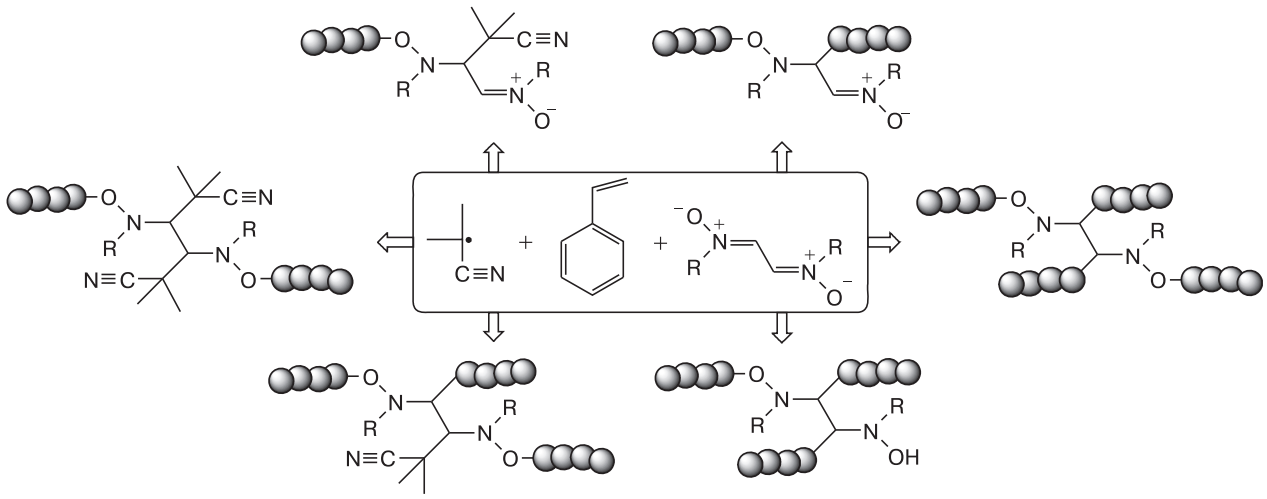

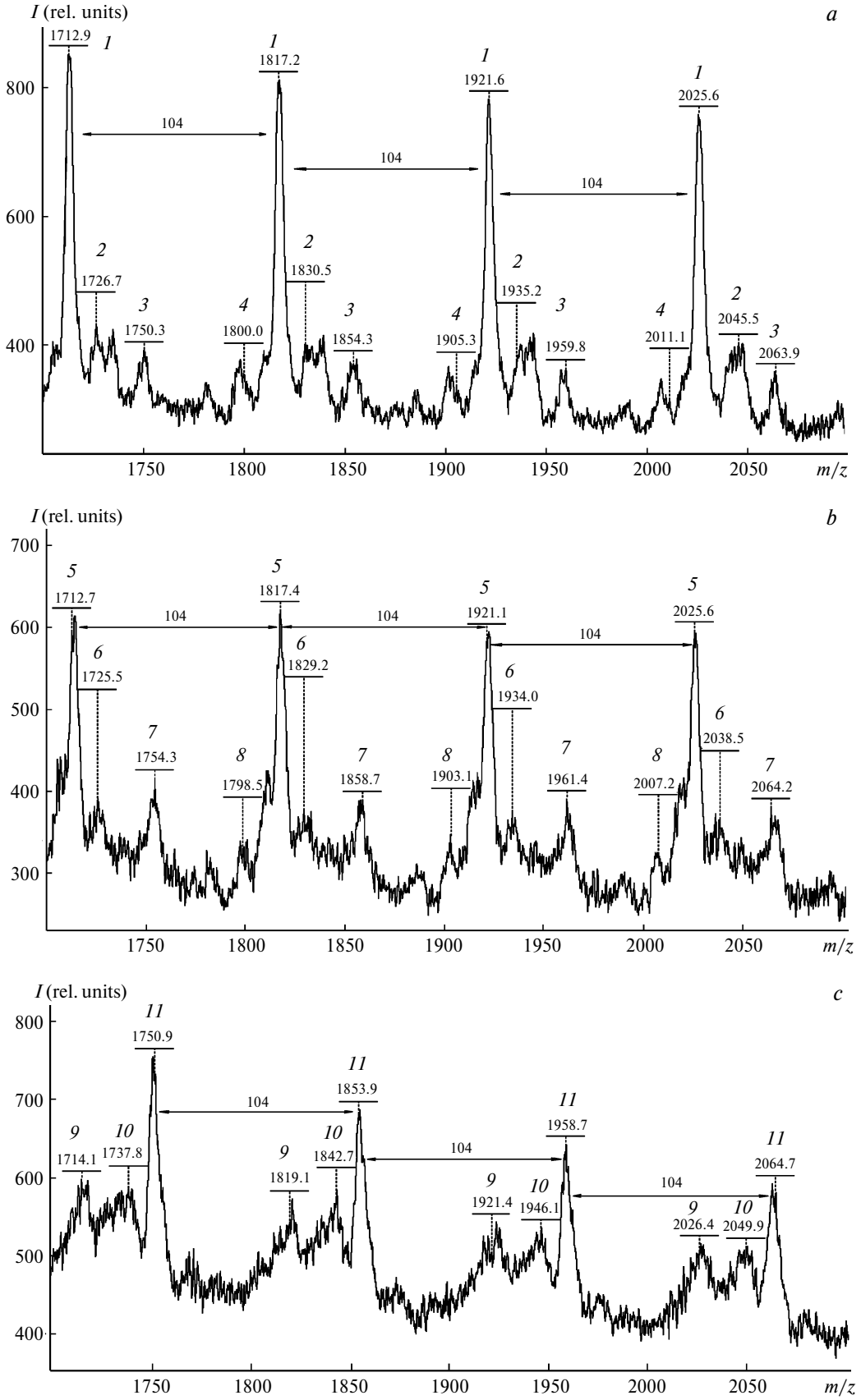

Fig. 2. MALDI-TOF mass spectra (m/z range 1700—2100 Da) of polystyrene ($M_n = 6000$, $M_w/M_n = 4.51$) synthesized in the presence of MDN (3 mol.%) and AIBN (1 mol.%) at 90 °C: DHB matrix, no salt (*a*) and DCTB matrix, with Ag salt (*b*); and of HAA ($M_w = 7600$, $M_w/M_n = 3.95$) synthesized in the presence of MDN and modified in the presence of CBr_4 at 130 °C: DCTB matrix, with Ag salt (*c*).

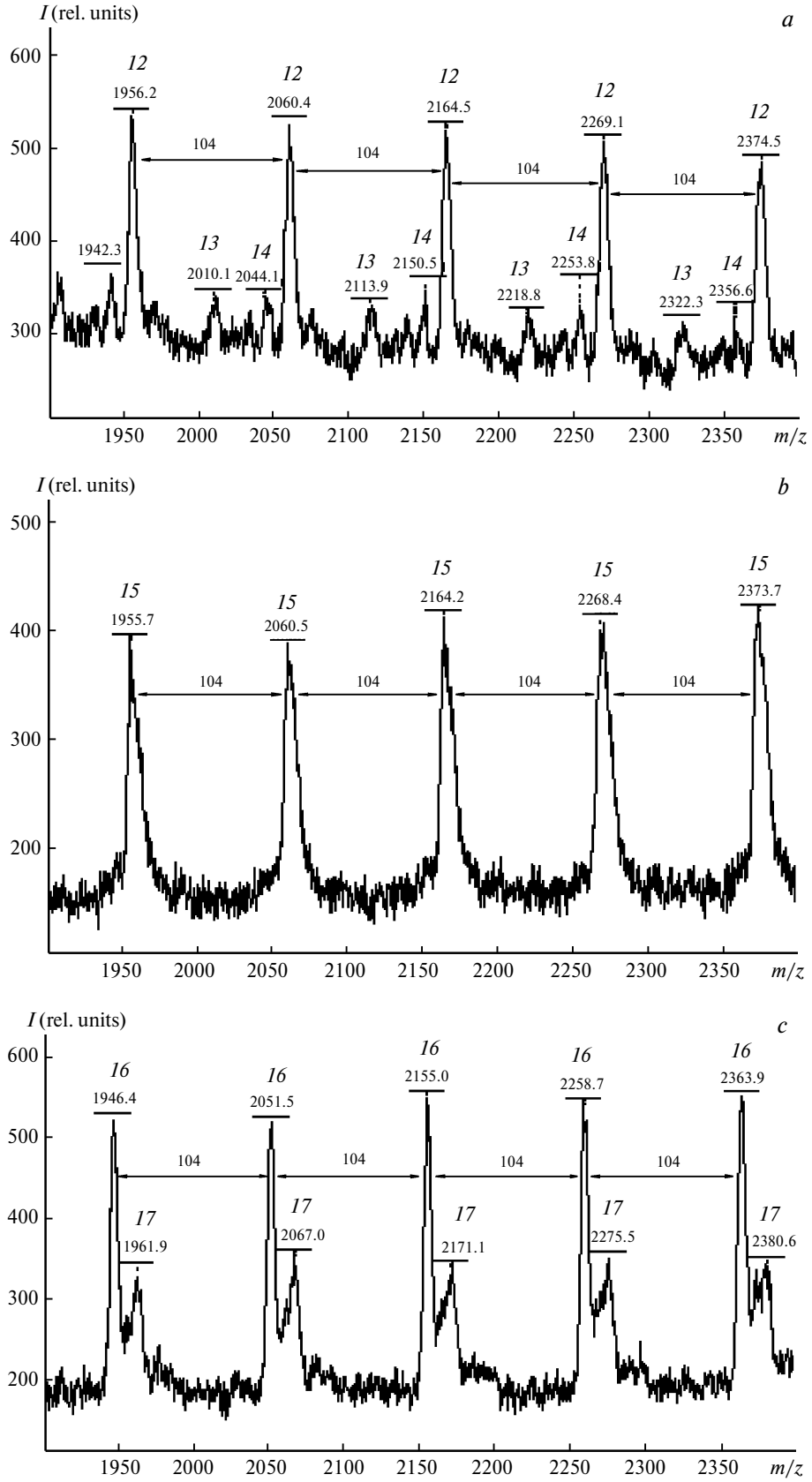

Fig. 3. MALDI-TOF mass spectra (m/z range 1900—2400 Da) of polystyrene ($M_n = 4200$, $M_w/M_n = 1.38$) synthesized in the presence of BDN (3 mol.%) and AIBN (1 mol.%) at 90 °C: DHB matrix (*a*); DCTB matrix, with Ag salt (*b*); and of HAA ($M_w = 3100$, $M_w/M_n = 1.47$) synthesized in the presence of BDN and mofidied in the presence of CBr_4 at 110 °C: DCTB matrix, with Ag salt (*c*).

Table 1. Structures corresponding to peaks in the MALDI-TOF mass spectra (see Figs 2 and 3) of MDN- and BDN-based HAAs and modified products

Figure	Dinitrone	Peak	Structure[a]	MW_{theor}/Da	MM_{exp}/Da
Fig. 2, *a*	MDN	*4*	$MDN(AIBN)_2(ST)_{15}C_6H_5CH_2H^+$	1906.7	1905.3
Fig. 2, *a*	MDN	*1*	$MDN(AIBN)_2(ST)_{16}H^+$	1919.8	1921.6
Fig. 2, *a*	MDN	*2*	$MDN(AIBN)_2(ST)_{16}CH_2H^+$	1933.8	1935.2
Fig. 2, *a*	MDN	*3*	$(AIBN)(ST)_{18}CH_2H^+$	1957.9	1959.8
Fig. 2, *b*	MDN	*8*	$MDN(AIBN)_2(ST)_{14}C_6H_5CH_2Ag$	1909.4	1903.1
Fig. 2, *b*	MDN	*5*	$MDN(AIBN)_2(ST)_{15}Ag^+$	1922.5	1921.1
Fig. 2, *b*	MDN	*6*	$MDN(AIBN)_2(ST)_{15}CH_2Ag^+$	1936.5	1934.0
Fig. 2, *b*	MDN	*7*	$(AIBN)(ST)_{17}CH_2Ag^+$	1960.6	1961.4
Fig. 2, *c*	MDN[b]	*9*	$MDN(AIBN)_2(ST)_{15}Ag^+$	1922.5	1921.4
Fig. 2, *c*	MDN[b]	*9*	$(AIBN)(ST)_{16}BrAg^+$	1922.3	1921.4
Fig. 2, *c*	MDN[b]	*10*	$(AIBN)(ST)_{17}Ag^+$	1946.6	1946.1
Fig. 2, *c*	MDN[b]	*11*	$(AIBN)(ST)_{17}Ag^+$	1960.6	1958.7
Fig. 2, *c*	MDN[b]	*11*	$MDN(AIBN)(ST)_{16}Ag^+$	1958.5	1958.7
Fig. 3, *a*	BDN	*12*	$(AIBN)(ST)_{18}CH_2H^+$	1957.9	1956.2
Fig. 3, *a*	BDN	*13*	$(BDN)_{0.5}(AIBN)_2(ST)_{17}H^+$	2007.9	2010.1
Fig. 3, *a*	BDN	*14*	$(AIBN)(ST)_{19}H^+$	2048.0	2044.1
Fig. 3, *b*	BDN	*15*	$(AIBN)(ST)_{17}CH_2Ag^+$	1960.6	1955.7
Fig. 3, *c*	BDN[b]	*16*	$(AIBN)(ST)_{17}Ag^+$	1946.6	1946.6
Fig. 3, *c*	BDN[b]	*17*	$(AIBN)(ST)_{17}CH_2Ag^+$	1960.6	1961.9

[a] Here (AIBN) stands for cyanopropyl radical (C_4H_6N), (ST) stands for C_8H_8; MDN stands for $(CH_3NOCH)_2$; and BDN stands for $(C(CH_3)_3NOCH)_2$.
[b] HAA modified in the presence of CBr_4.

MALDI-TOF mass spectra represent series of main signals (Fig. 2, *a*, signals *1*; Fig. 2, *b*, signals *5*) characteristic of the HAA containing MDN and two cyanoisopropyl groups. The weaker signals observed with a period of 104.15 Da using both matrices (Fig. 2, *a*, signals *2—4*; Fig. 2, *b*, signals *6—8*, Table 1) correspond to decomposition products of the MDN-containing macromolecules under the MALDI ionization conditions. The main decomposition channels of the PS chain containing no DNs are presented in Scheme 2.

Figure 3, *a* demonstrates the MALDI-TOF mass spectrum of PS synthesized in the presence of BDN. It was recorded using the DHB matrix. In contrast to the MALDI-TOF mass spectrum of the MDN-containing HAA the spectrum of PS synthesized using BDN-mediated polymerization exhibits one strong signal (signal *12*) corresponding to the product of PS decomposition under the MALDI ionization conditions (see Table 1, Scheme 2). In addition, there are two weak, nearly background-level signals separated by an interval of 104.15 Da. Signal *13*

Scheme 2

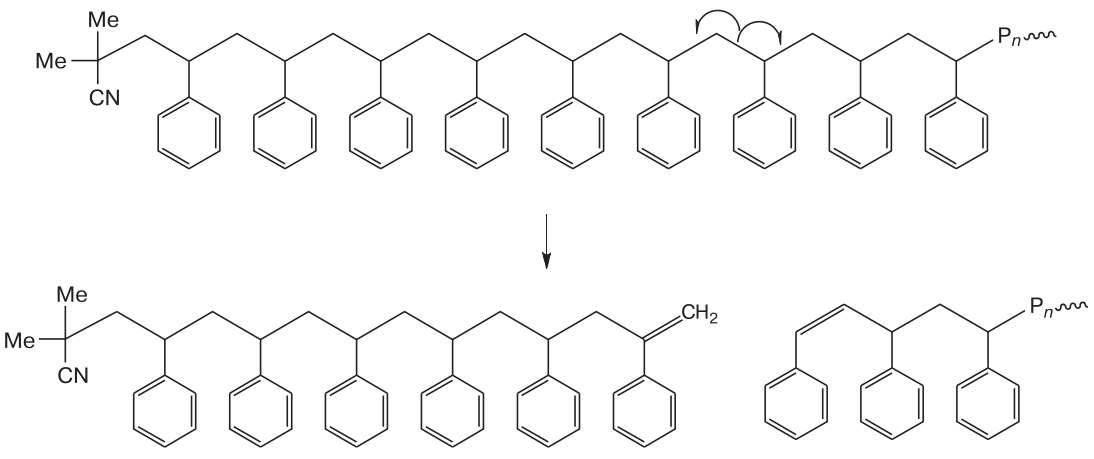

Scheme 3

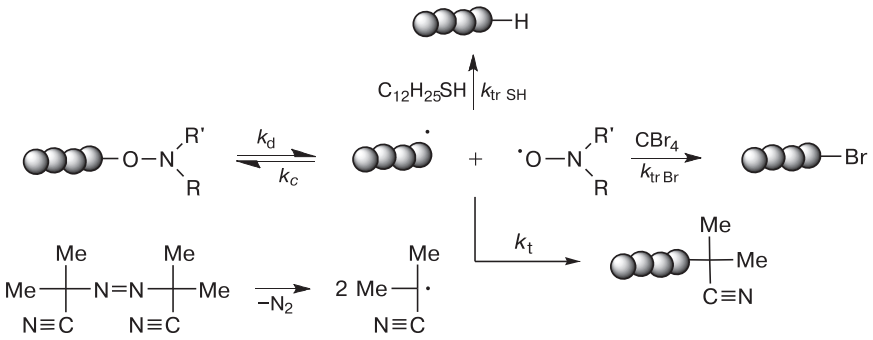

corresponds to a single-nitroxide product of HAA decomposition at the C—C bond in the DN molecule while signal *14* corresponds to the protonated polystyrene chain. The MALDI-TOF mass spectrum of the BDN-based HAA recorded using the DCTB matrix (see Fig. 3, *b*) is similar to the spectrum recorded using the DHB matrix, which also exhibits one main peak (*15*) corresponding to the polystyrene chain (see Scheme 2) formed upon the decomposition of HAA. Indeed, BDN-based nitroxide radicals are unstable under UV irradiation and decompose to MNP and *tert*-butyl vinyl nitroxides at high temperatures.[38] Therefore, the decomposition products observed in the MALDI-TOF mass spectra of the BDN-based HAA can form both during the polymerization and under the ionization conditions of the polymer samples.

The results of the MALDI-TOF analysis unambiguously demonstrate the presence of nitroxide moieties in the HAAs but give no structural information. In particular, the question about location of the nitroxide fragment in the polymer chain (as terminal group or within the chain) remains unanswered. To analyze the structure of the polymers synthesized in the presence of α-DNs in more detail, we modified them in the presence of chain transfer agents (dodecyl mercaptane $C_{12}H_{25}SH$, CBr_4) and studied thermal decomposition of the HAAs followed by chain termination on different inhibitors (atmospheric oxygen; 4,5,5-trimethyl-2,2-diethyl-2,5-dihydroimidazole-1-oxide (nitroxide N); 3,5-di-*tert*-butylbenzoquinone-1,2 (35Q)) and on a cyanoisopropyl radical generated during the decomposition of azobisisobutyronitrile (AIBN) (Scheme 3). Preliminary studies showed that modification of HAAs takes 20 h at 90 °C and 7 h at 130 °C to complete. No further decrease in the MW of the HAAs was observed at longer times.

Location of the nitroxide fragment in the HAAs was assessed from the decrease in the MW of the modified polymers compared to the starting unmodified polymers, in particular, from the MW values corresponding to the peak on the MW distribution (MWD) curve (M_p, see Tables 2—4). Note that the decomposition and modification of the HAAs based on α-DNs containing intramolecular nitroxide moieties should be accompanied by a decrease in the MW of the end product (Scheme 4, reactions 2—4). The MW characteristics of low-molecular-weight AAs and HAAs with terminal nitroxide group (see Scheme 4, reaction 1) should remain unchanged.

The MDN-containing PS was modified in the presence of CBr_4 as efficient chain transfer agent (chain transfer constant is 2.2 at 60 °C, see Ref. 40) and various inhibitors of radical processes including 35Q, atmospheric oxygen, and the nitroxide radical (nitroxide N) at 130 °C. This temperature range is optimum for carrying out MDN-

Table 2. Molecular weight characteristics of the thermolysis and modification products of the HAAs synthesized *in situ* in the presence of AIBN (1 mol.%) and MDN (0.5 mol.%)

Run	Components	*T*/°C	t_{mod}[a]/h	$M_n \cdot 10^{-3}$	$M_w \cdot 10^{-3}$	M_w/M_n	ΔM_w
1	Unmodified **1**	90	—	3.8	9.3	2.45	—
2	**1**, CBr_4, THF	130	7	3.7	5.5	1.49	3800
3	**1**, 35Q, THF	130	7	4.4	6.0	1.36	3300
4	**1**, O_2, DMSO	130	7	3.3	7.2	2.18	2100
5	**1**, N, O_2, DMSO	130	7	4.3	7.6	1.77	1700
6	Unmodified **2**	90	—	10.5	47.2	4.50	—
7	**2**, CBr_4, C_6H_6	130	7	8.6	30.6	3.55	17000
8	**2**, O_2, DMSO	130	7	11.0	35.5	3.22	11700

[a] t_{mod} is the HAA modification time or the thermolysis time.

Scheme 4

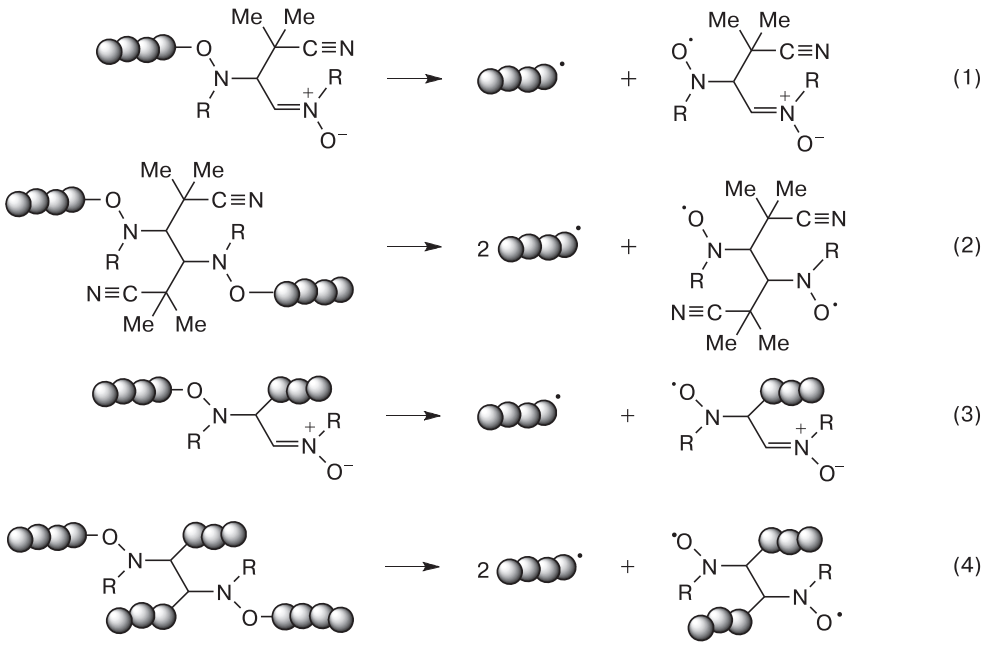

Table 3. Molecular weight characteristics of the thermolysis and modification products of the HAAs synthesized *in situ* in the presence of AIBN (1 mol.%) and BDN (0.5 mol.%)

Run	Components	T/°C	t_{mod}/h	$M_n \cdot 10^{-3}$	$M_w \cdot 10^{-3}$	$M_p \cdot 10^{-3}$	M_w/M_n	ΔM_w	ΔM_p
1[a]	Unmodified **3**	90	—	4.2	5.8	4.8	1.38	—	—
2	**3**, CBr_4, C_6H_6	110	20	3.1	4.6	4.0	1.48	1200	800
3	**3**, $C_{12}H_{25}SH$, C_6H_6	110	20	1.9	4.7	4.1	2.47	1100	700
4	Unmodified **4**	90	—	7.8	12.7	11.0	1.63	—	—
5	**4**, CBr_4, C_6H_6	110	20	5.8	10.6	9.0	1.83	2100	2000
6	**4**, $C_{12}H_{25}SH$, C_6H_6	110	20	7.0	10.3	8.6	1.47	2400	2400
7	Unmodified **5**	90	—	8.6	14.8	13.9	1.72	—	—
8	**5**, CBr_4, THF	130	7	7.7	12.5	10.4	1.62	2300	3500
9	**5**, 35Q, THF	130	7	8.6	13.3	11.0	1.54	1500	2900
10	**5**, O_2, DMSO	130	7	7.8	13.0	10.9	1.67	1800	3000
11	**5**, N, O_2, DMSO	130	7	7.3	12.6	10.5	1.73	2200	3400
12	Unmodified **6**	90	—	10.8	20.5	16.6	1.90	—	—
13	**6**, AIBN, C_6H_6	90	20	10.1	18.8	15.6	1.86	1700	1000
14	**6**, CBr_4, C_6H_6	110	20	7.8	16.2	13.4	2.07	4300	3200
15	**6**, $C_{12}H_{25}SH$, C_6H_6	110	20	9.6	16.3	13.9	1.70	4200	2700
16	**6**, CBr_4, THF	130	7	9.5	16.1	13.1	1.69	4400	3500
17	**6**, 35Q, THF	130	7	9.8	16.6	13.6	1.69	3900	3000
18	**6**, O_2, DMSO	130	7	9.3	17.2	14.1	1.83	3300	2500
19	**6**, N, O_2, DMSO	130	7	9.3	16.4	12.6	1.76	4100	4000
20	Unmodified **7**	70	—	23.1	52.4	36.6	2.27	—	—
21	**7**, AIBN, C_6H_6	90	20	19.3	47.0	32.5	2.44	5400	4100
22	**7**, CBr_4, C_6H_6	110	20	14.6	42.0	27.3	2.87	10400	9300
23	**7**, $C_{12}H_{25}SH$, C_6H_6	110	20	17.6	43.0	28.3	2.44	9400	8300
24	**7**, CBr_4, THF	130	7	14.9	38.8	25.6	2.60	13200	11000
25	**7**, 35Q, THF	130	7	16.8	40.4	25.2	2.40	12000	11400
26	**7**, O_2, DMSO	130	7	15.2	40.2	26.2	2.64	12200	10400
27	**7**, N, O_2, DMSO	130	7	13.5	30.5	19.9	2.25	21900	16700

[a] HAA synthesized in the presence of BDN (3 mol.%).

Table 4. Molecular weight characteristics of products thermolysis and modification of HAA synthesized *in situ* in the presence of AIBN (1 mol.%) and PDN (0.5 mol.%)

Run	Components	T/°C	t_{mod}/h	$M_n \cdot 10^{-3}$	$M_w \cdot 10^{-3}$	$M_p \cdot 10^{-3}$	M_w/M_n	ΔM_w	ΔM_p
1	Unmodified **8**	90	—	10.7	19.1	17.0	1.79	—	—
2	**8**, AIBN, C_6H_6	90	20	10.1	18.0	15.9	1.78	1100	1100
3	**8**, CBr_4, C_6H_6	90	20	9.6	17.7	15.9	1.84	1400	1100
4	**8**, $C_{12}H_{25}SH$, C_6H_6	90	20	10.8	17.9	16.8	1.66	1200	200
5	**8**, CBr_4, TGF	130	7	11.0	17.1	15.6	1.55	2000	1400
6	**8**, O_2, DMSO	130	7	10.2	17.2	15.8	1.69	1900	1200
7	**8**, N, O_2, DMSO	130	7	9.0	16.0	12.8	1.78	3100	4200
8[a]	Unmodified **9**	90	—	13.9	28.8	24.4	2.08	—	—
9	**9**, AIBN, C_6H_6	90	20	14.0	28.3	24.0	2.02	500	400
10	**9**, CBr_4, C_6H_6	90	20	13.6	27.4	23.7	2.01	1400	700
11	**9**, $C_{12}H_{25}SH$, C_6H_6	90	20	14.6	27.7	23.8	1.90	1100	600
12	Unmodified **10**	90	—	18.0	52.7	28.9	2.93	—	—
13	**10**, AIBN, C_6H_6	90	20	19.3	53.4	28.9	2.76	—	—
14	**10**, CBr_4, C_6H_6	90	20	18.9	52.0	29.5	2.75	700	—
15	**10**, $C_{12}H_{25}SH$, C_6H_6	90	20	19.5	52.5	29.5	2.70	200	—
16	Unmodified **11**	70	—	38.9	88.0	71.7	2.26	—	—
17	**11**, AIBN, C_6H_6	90	20	41.0	87.1	71.7	2.12	900	—
18	**11**, CBr_4, C_6H_6	90	20	37.7	85.5	70.5	2.27	2500	1200
19	**11**, CBr_4, TGF	130	7	45.6	82.5	68.0	1.80	5500	3700
20	**11**, 35Q, TGF	130	7	41.4	80.8	68.2	1.95	7200	3500
21	**11**, O_2, DMSO	130	7	33.3	80.0	70.1	2.40	8000	1600
22	**11**, N, O_2, DMSO	130	7	25.6	73.4	67.3	2.87	14600	3800

[a] HAA synthesized in the presence of PDN (3 mol.%).

mediated CRP of PS in the reversible inhibition regime.[20] Therefore, decomposition of MDN-based HAAs will proceed with the highest efficiency under these conditions. Changes in MW were evaluated from the M_w values treated as the most reliable experimental data. The modified products based on the PS samples synthesized in the presence of MDN (0.5 mol.%) and isolated at different ST conversions (samples **1** and **2**) demonstrated a decrease in their MWs (see Table 2). In the course of modification or thermolysis the corresponding MWD curves are shifted toward lower MW values (Fig. 4). Noteworthy, as the MW of the starting PS sample increases from 3.8 (sample **1**) to 10.5 kDa (sample **2**), the corresponding M_w difference also increases. This can be indicative of either migration of the nitroxide fragment toward the mid-point of the polymer chain during MDN-mediated polymerization of styrene or possible formation of a star-shaped polymer whose decomposition produces two polymer chains (see Scheme 4, reaction 4). It should be noted that modification of the HAAs synthesized under identical conditions but isolated at different monomer conversions (see Table 2, *cf.* runs 2 and 7, 4 and 8) is accompanied by changes in the MWs of both decomposition products (see Table 2, columns "M_w" and "ΔM_w"). The increase in the MWs of both decomposition products including the nitroxide one can suggest that the initial stage of the process mainly involves the formation of linear polymers that undergo transformation to four-arm star-shaped structures (see Scheme 4, reactions 3 and 4).

Structure determination of the modified HAA sample was performed by MALDI-TOF mass spectrometry using the DCTB matrix and the silver salt (see Fig. 2, *c*). This MALDI-TOF mass spectrum differs from that of the starting unmodified MDN-containing PS (see Fig. 2, *b*). The

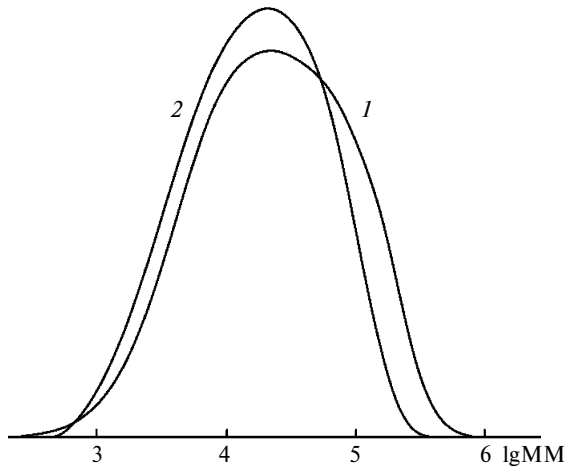

Fig. 4. Molecular weight distribution curves of polystyrene synthesized in the presence of MDN (0.5 mol.%) and AIBN (1 mol.%) at 90 °C: umodified PS sample with M_n = 10500 Da (*1*) and PS modified in the presence of CBr_4 at 130 °C (*2*).

MALDI-TOF mass spectrum of the PS sample modified in the presence of CBr_4 exhibits three peaks. One of them corresponds to the starting MDN-containing polymer (signal *9*) while the other two peaks (signals *10* and *11*) correspond to the HAA decomposition products. Note that signal *11* can correspond to two structures of the HAA decomposition products (see Table 1). Besides, peak *9* can also correspond to the bromine-containing polymer chain. By and large, the intensities of these signals unambiguously prove the HAA decomposition at the C—O bond of the polymer—nitroxide group fragment under the modification conditions.

Modification of PS was studied in detail taking the BDN-containing HAA as an example. A total of five PS samples with $4.2 < M_n < 23.1$ kDa (samples **3**—**7**, see Table 3) and a number of modifiers (AIBN, $C_{12}H_{25}SH$) were studied. The temperature range of the modification and thermolysis processes was extended to 90—130 °C. It was established that, similarly to the MDN-containing HAA, decomposition of the BDN-based PS also efficiently proceeds at 130 °C. However, decomposition at the C—O bond in the HAA molecule can also proceed under milder conditions (at 90—110 °C). For instance, the MW of the modified sample decreases at 90 °C in the presence of AIBN in contrast to the MW of the starting unmodified sample. Modification and thermolysis proceed most efficiently in the presence of CBr_4 and nitroxide N and atmospheric oxygen. As the MW of the starting PS increases, the MW difference between the starting and modified product slightly increases, being most pronounced for the modification of PS ($M_n = 23100$) synthesized at 70 °C. It follows that the nitroxide moiety in the PS sample with the higher M_n is closer to the mid-point of the polymer chain. In addition, as in the case of the MDN-based samples, the MWs of the decomposition products of the samples isolated at different monomer conversions change (see Table 3, *cf.* modification of samples **5** and **6**, runs 8 and 16). This also suggests a gradual transformation of the two-arm structures to four-arm ones.

Figure 5 presents the MWD curves of the BDN-based HAA and a product of thermolysis in the presence of nitroxide N and atmospheric oxygen. The MWD curve is noticeably shifted toward lower MW values. By and large, the results of modification and thermolysis of BDN-based HAA show that the nitroxide moiety is located within the polymer chain.

Differences between the MALDI-TOF mass spectrum of the PS sample obtained by BDN-mediated polymerization and modified in the presence of CBr_4 in a benzene solution and the spectrum of the unmodified PS sample (see Fig. 3, *b*, *c*) are less pronounced than for the MDN-containing samples. In particular, the MALDI-TOF mass spectrum of the modified sample exhibits two intense peaks (signals *16* and *17*, see Fig. 3, *c* and Table 1) corresponding to decomposition products of the PS sample (see

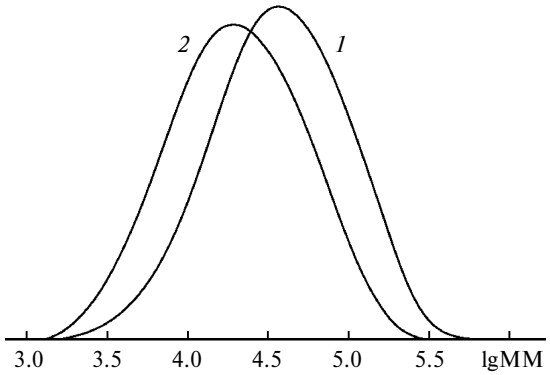

Fig. 5. Molecular weight distribution curves of polystyrene synthesized in the presence of BDN (0.5 mol.%) and AIBN (1 mol.%): unmodified PS sample with $M_n = 23100$ Da (*1*) and PS ($M_n = 13500$ Da) modified in the presence of nitroxide N and atmospheric oxygen in DMSO solution (*2*).

Fig. 3, *c*). Coincidence of the signals in the MALDI-TOF mass spectra of the unmodified sample (Fig. 3, *b*) and the modified product (Fig. 3, *c*), as well as the decrease in the MW of the BDN-based HAA under the modification conditions (90—130 °C) is indicative of the decomposition of HAA under MALDI ionization conditions. Modification of the PDN-containing HAA led to somewhat different results compared to those obtained for the MDN- and BDN-based HAAs. Earlier,[20] we found that PDN influences the kinetics of ST polymerization and the MW characteristics of the polymers to a lesser extent. Indeed, PDN-mediated polymerization affords macromolecules with higher MW from 10.7 to 38.9 kDa (samples **8**—**11**). It was shown that modification and thermolysis of these samples at 90 °C causes a slight decrease in the MW of the HAA and that the MW difference between the unmodified and modified samples can be comparable with the error in MW determination by GPC (see Table 4). Raising the temperature of (i) modification in the presence of CBr_4 and (ii) thermolysis in the presence of atmospheric oxygen and nitroxide N or 35Q to 130 °C causes a greater increase in the MW difference between the unmodified PS and the modified product for both the sample with $M_n = 10700$ (see Table 4, runs 5—7) and the higher-molecular-weight AA (see Table 4, runs 19—22). However, in contrast to the MDN- and BDN-based HAAs, the shift of the MWD curves of the PDN-containing HAA toward lower MWs is less pronounced (see Figs 4—6), although a shoulder is formed in the lower-MW region.

Thus, a MALDI-TOF mass spectrometric and GPC analysis of HAAs as well as modification and thermolysis of these compounds made it possible to determine the structure of both untreated and modified PS samples and to assess the location of the nitroxide moiety in the macromolecules. In particular, HAAs obtained by MDN- and BDN-mediated polymerization of ST contain the nitrox-

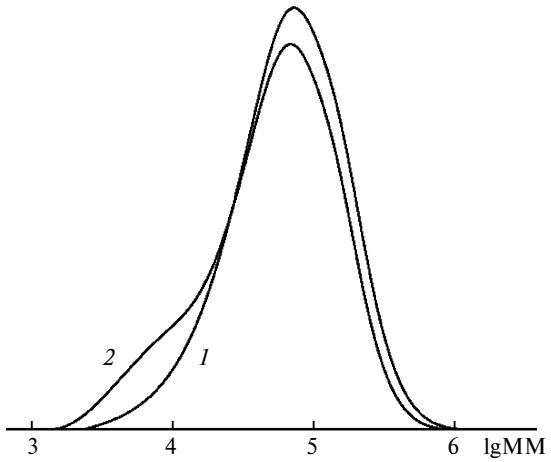

Fig. 6. Molecular weight distribution curves of polystyrene synthesized in the presence of PDN (3 mol.%) and AIBN (1 mol.%) at 90 °C: unmodified PS sample with M_n = 38900 Da (*1*) and PS modified in the presence of atmospheric oxygen and nitroxide N (*2*).

ide fragment within the polymer chain. Changes in the MWs of both decomposition products of the HAAs isolated at different monomer conversions (see above) also provide indirect evidence of formation of star-shaped structures.

Hydrodynamic and conformational characteristics of polystyrene macromolecules synthesized in the presence of α-dinitrones. Theoretically, the use of α-DNs as mediators of *in situ* polymerization of ST allows one to synthesize branched polymers (three- and four-arm star-shaped polymers, see Scheme 1). As mentioned above, steric hindrances produced by substituents in the DN molecules can govern the formation of macromolecules having a particular configuration. The results of the MALDI-TOF mass spectrometric and GPC analyses of PS do not provide unambiguous information on the topology of macromolecules. In particular, BDN-containing HAAs decompose under MALDI ionization conditions (see above). The MDN-based HAAs contain the nitrone group and two cyanoisopropyl groups. Note that DN-mediated synthesis of PS at 90 °C and at higher temperatures can be initiated not only by an initiator, but also thermally.[41] The initiating radical (product of a Diels—Alder reaction) will correspond to the doubled MW of styrene; thus unambiguous determination of the HAA structure and the more so the topological features of the macromolecules by MALDI-TOF mass spectrometry is impossible. To this end, we studied a number of hydrodynamic parameters of macromolecules that allow one to better assess the architecture of the PS samples. Table 5 presents the synthesis conditions for and the MW characteristics of the DN-based PS samples studied in this Section.

The M_w values were determined from the Debye equation (1) and by the double extrapolation method from the Debye—Zimm equation (2) using the static light scattering data. The viscosity-average MWs (M_η) are listed in Table 5.

$$\frac{K \cdot c}{R_\theta} = \frac{1}{M_w} + 2A_2 \cdot c, \qquad (1)$$

where K is the optical constant

$$K = \frac{4\pi^2 n_0^2}{N_A \lambda_0^4}\left(\frac{dn}{dc}\right)^2,$$

c is the solution concentration; R_θ is the Rayleigh ratio of the excess intensity of light scattered at an angle of 90°; A_2 is the second virial coefficient; N_A is the Avogadro constant, λ_0 is the wavelength of incident light, n_0 is the refractive index of the solvent, n is the refractive index of the solution, and dn/dc is the refractive index increment

$$\frac{K \cdot c}{R_\theta} = \frac{1}{M_w}\left\{1 + \frac{16\pi^2 n_0^2}{3\lambda_0^2} \cdot \overline{R_g^2} \cdot \sin^2\frac{\theta}{2}\right\} + 2A_2 \cdot c, \qquad (2)$$

where θ is the light scattering angle and R_g is the radius of gyration.

Table 5. Synthesis (90 °C, with AIBN (1 mol.%) as initiator) and molecular weight characteristics of PS samples

Sample no.	Dinitrone	*t*/h	S[a] (%)	GPC			$M_\eta \cdot 10^{-3}$	$M_w \cdot 10^{-3}$ from light scattering data	
				$M_n \cdot 10^{-3}$	$M_w \cdot 10^{-3}$	M_w/M_n		Debye	Zimm
1[b]	—	2	32	25.5	45.8	1.8	—	51.1	51.2
2	—	1.3	87	17.6	64.5	3.67	64.4	—	—
3	MDN (0.5)	25.3	85	11.6	64.4	5.57	49.4	72.1	72.7
4	MDN (3.0)	5.0	77	9.8	26.6	2.72	26.2	38.1	38.8
5	BDN (0.5)	10.0	68	12.3	23.1	1.86	21.7	27.5	27.3
6	BDN (1.5)	150.0	61	8.0	14.0	1.75	15.4	26.0	26.0
7	PDN (0.5)	2.0	83	16.0	39.4	2.46	31.8	49.3	49.6
8	PDN (3.0)	47.5	68	14.9	30.6	2.06	24.8	32.1	33.1

[a] *S* stands for monomer conversion.
[b] Sample synthesized at 110 °C.

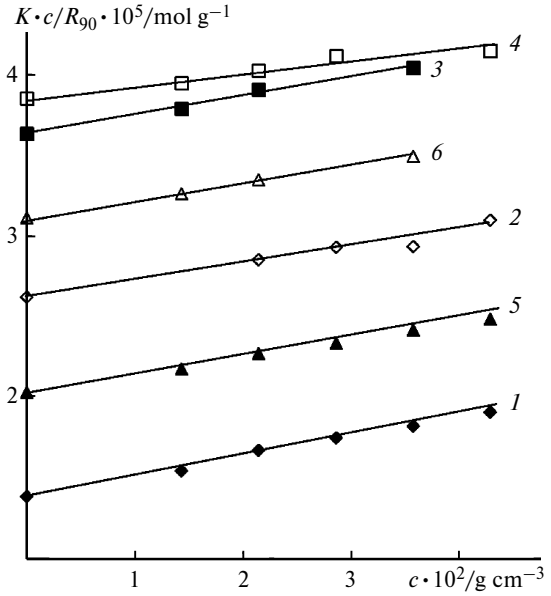

Fig. 7. Concentration dependences of the inverse intensity of scattered light Kc/R_{90} for solutions of polystyrene synthesized by DN-mediated polymerization in toluene: 0.5 mol.% MDN (*1*); 3 mol.% MDN (*2*); 0.5 mol.% BDN (*3*); 1.5 mol.% BDN (*4*); 0.5 mol.% PDN (*5*); and 3 mol.% PDN (*6*).

Figure 7 presents the dependences of the inverse intensity of scattered light $(K \cdot c)/R_{90}$ on the concentration c of the studied PS samples. These are linear plots characteristic of dilute polymer solutions. The Y-intercept equals $1/M_w$ while the slope equals the doubled second virial coefficient A_2 (see Table 6). As should be expected, the A_2 coefficient for the toluene—PS system is positive and rather large, being characteristic of thermodynamically good solvents.

The double extrapolation method is more accurate and allows one to calculate the MW of a polymer ignoring the macromolecular conformations in solution, the A_2 coefficient, and the radius of gyration of the macromolecule based on the Zimm plot (Fig. 8).

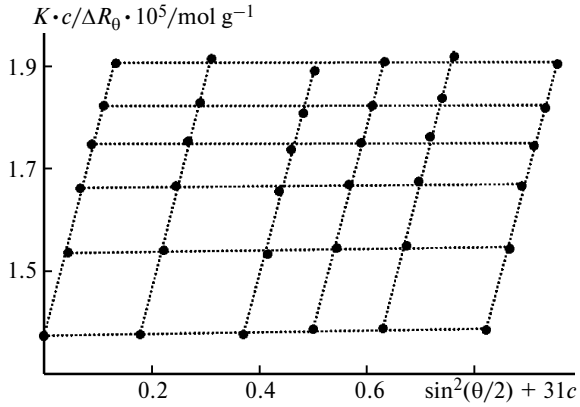

Fig. 8. Zimm double extrapolation plot taken over concentration (c) and angle (θ) for solution of polystyrene sample synthesized in the presence of MDN (0.5 mol.%).

Figure 9 presents the concentration dependences of the reduced viscosity η_{sp}/c for the PS solutions. They were analyzed using the Huggins equation (3):

$$\frac{\eta_{sp}}{c} = [\eta] + k'[\eta]^2 c, \qquad (3)$$

where k' is the Huggins constant that characterizes the thermodynamic interaction polymer—solvent and the hydrodynamic behavior of the solution.

The calculated k' values of the PS samples synthesized in the presence of α-DN are listed in Table 6. The constant k' allows one to evaluate the affinity between the polymer and solvent. The larger the difference between the nature of solution components the larger the constant k'. The lower the quality of the solvent the larger the number of encounters between macromolecules and the larger the Huggins constant. The Huggins constants of the PS samples synthesized using both the conventional initiator and DNs fall in the range from 0.08 to 0.33 (see Table 6). These values as well as the A_2 values also suggest good solubility of all PS samples in toluene.

Table 6. Molecular weight and hydrodynamic characteristics of polystyrene samples

Run	DNs (mol.%)	M_w[a] $\cdot 10^{-3}$	$A_2 \cdot 10^4$ /cm^3 mol g^{-2}	[η] /cm^3 g^{-1}	k'	$D_0 \cdot 10^7$ /cm^2 s^{-1}	R_g	R_{h-D}	$R_{h-\eta}$	ρ	g'	$(R_g^2/M_w) \cdot 10^3$ /nm^2 mol^{-1}
							nm				/nm	
1	—	51.0	6.06	—	—	—	9.8	—	6.2	—	0.99	1.88
2[b]	—	64.4	—	35.4	0.12	—	—	—	7.1	—	0.99	—
3	MDN (0.5)	72.7	6.30	29.5	0.18	4.6	6.6	8.5	7.0	0.78	0.77	0.60
4	MDN (3.0)	38.8	3.50	19.0	0.18	6.4	8.4	6.1	4.9	1.38	0.76	1.82
5	BDN (0.5)	27.3	3.01	16.7	0.33	7.3	10.1	5.4	4.2	1.87	0.86	3.74
6	BDN (1.5)	26.0	4.49	13.2	0.16	7.3	8.8	5.4	3.8	1.63	0.69	2.98
7	PDN (0.5)	49.6	5.51	21.7	0.15	4.3	9.0	9.0	5.6	1.00	0.73	1.63
8	PDN (3.0)	33.1	5.20	18.3	0.08	6.1	9.6	6.5	4.6	1.48	0.82	2.78

[a] MW was determined from the Zimm plot.
[b] The viscosity-average MW; $\rho = R_g/R_{h-D}$; $g' = [\eta]_{br}/[\eta]_{lin}$.

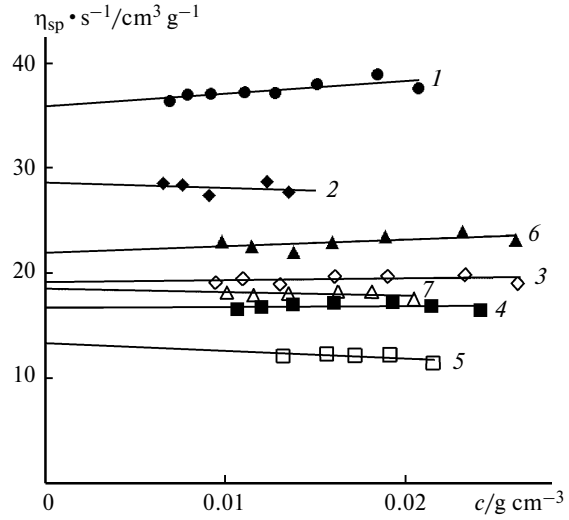

Fig. 9. Reduced viscosity η_{sp}/c plotted *vs*. concentration c of solution of polystyrene synthesized under DN-free conditions (*1*) and in the presence of dinitrones: 0.5 mol.% MDN (*2*); 3 mol.% MDN (*3*); 0.5 mol.% BDN (*4*); 1.5 mol.% BDN (*5*); 0.5 mol.% PDN (*6*); and 3 mol.% PDN (*7*).

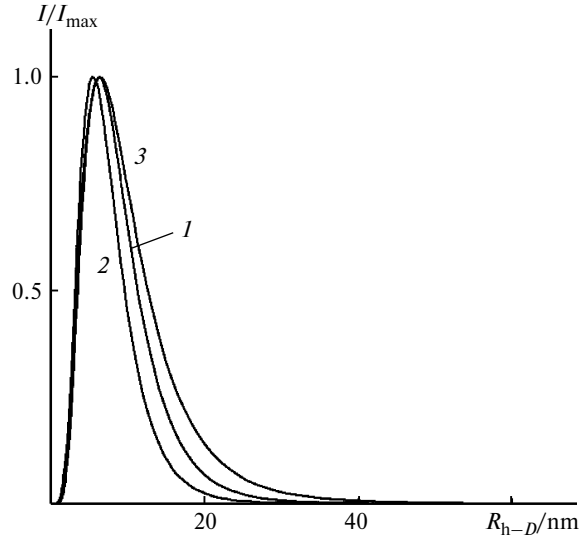

Fig. 10. Plots of relative light intensity I/I_{max} *vs*. hydrodynamic size R_h of scattering particles for solutions of PS synthesized in the presence of AIBN (1 mol.%) and different dinitrones (3 mol.%): MDN (*1*), BDN (*2*), and PDN (*3*).

The intrinsic viscosity [η] values of the PS samples calculated from the Mark—Kuhn—Houwink equation (4)

$$[\eta] = K \cdot M^a, \quad (4)$$

where $K = 17 \cdot 10^{-3}$ and $a = 0.69$ at 25 °C (see Ref. 42) were used to determine the M_η values (see Table 5).

The viscosity-average MWs of the PS samples fall in the range from M_n to M_w. Note that the MWs of the PS samples calculated using the Debye—Zimm plot are in very good agreement and differ only slightly. Contrary to this, the difference between the M_w values determined by GPC and by static light scattering is very large (see Table 5). The error in determination of these values for most PS samples synthesized in the presence of DNs can be as large as 15—20%. Underestimation of the M_w value determined by GPC compared to the true M_w value can be due to the formation of branched polymers in the presence of DNs. The M_w^{GPC} values depend on the hydrodynamic radius of macromolecules, which is usually smaller for branched molecules compared to linear ones.[43]

The hydrodynamic and conformational properties of macromolecules are in no small part due to the molecular architecture (types of branching, rigidity, and the size and number of arms). To study the configuration of PS macromolecules synthesized in the presence of α-DNs in more detail, these samples were characterized by dynamic light scattering. All PS solutions in toluene were characterized by one diffusion mode (Fig. 10) indicating the formation of true molecular solutions. The hydrodynamic radii, R_{h-D}, of macromolecules were evaluated using the Stokes—Einstein equation (5) and experimental data:

$$D_0 = \frac{k_B T}{6\pi\eta_0 R_{h-D}}, \quad (5)$$

where D_0 is the diffusion coefficient, k_B is the Boltzmann constant, T is absolute temperature, and η_0 is the viscosity of the solvent.

Using the [η] values, were also calculated the hydrodynamic radii of macromolecules from the Einstein formula:

$$[\eta] = 2.5 N_A \left(\frac{V}{M_w}\right) = \frac{\left(\frac{10\pi}{3}\right) N_A R_{h-\eta}^3}{M_w} \quad (6)$$

$$R_{h-\eta} = \left(\frac{3[\eta]M_w}{10\pi N_A}\right)^{\frac{1}{3}} \quad (7)$$

where $R_{h-\eta}$ is the viscosity hydrodynamic radius of the equivalent sphere (see Table 6); V is the volume of the sphere; and M_w is the MW of the polymer determined by static light scattering.

The data of Table 6 show that the viscosity hydrodynamic radii ($R_{h-\eta}$) of the PS samples synthesized in the presence of α-DNs are comparable with their diffusion hydrodynamic radii (R_{h-D}), being noticeably smaller than the latter. This is due to the fact that for these samples the principle of equivalence of the size of macromolecules for translational (diffusion and sedimentation) and rotational (intrinsic viscosity) motion is violated.

The hydrodynamic properties of polymers are governed by the density of the molecular coil. One should expect that branched and linear polymeric systems of the same

chemical nature will behave differently in solution. For instance, the structure of a macromolecule is characterized by the ratio of the hydrodynamic radius R_{h-D} to the radius of gyration R_g of the macromolecule, or the so-called ρ-parameter proposed by Burkhard, $\rho = R_g/R_{h-D}$ (see Table 6). It characterizes the degree of asymmetry of the macromolecule in solution. The ρ values for certain macromolecular conformations are available. It is commonly believed[44] that a hard sphere is characterized by $\rho = 0.778$ while a Gaussian coil of polydispersed linear polymer is characterized by $\rho = 1.73$ in θ-solvent and $\rho = 2.05$ in good solvent. Ellipsoids and rigid-rod polymers have $\rho > 2.05$. Four-arm polydispersed star-shaped polymers in θ-solvent are characterized by $\rho = 1.534$. An increase in the number of arms or branching points in the macromolecule causes the ρ-parameter to decrease to 1.225. The ρ-parameter of PS synthesized in the presence of BDN (0.5 mol.%) is close to that of the Gaussian coil of linear polydispersed polymer (see Table 6). The ρ-parameters of PS synthesized in the presence of MDN (0.5 mol.%) and PDN (0.5 mol.%) are close to that of a hard sphere or hyperbranched polymers. By and large, changes in the concentration of MDN, BDN, and PDN according to the analyzed parameter can lead to formation of branched and star-shaped polymers.

Branching in macromolecules is also evaluated using the so-called Zimm branching factor of the radius of gyration (g) and the Zimm branching factor of intrinsic viscosity (g')

$$g = \frac{R^2_{g_{br}}}{R^2_{g_{lin}}}, \quad (8)$$

$$g' = \frac{[\eta]_{br}}{[\eta]_{lin}}, \quad (9)$$

$$g' = g^b, \quad (10)$$

where $R_{g_{br}}$ and $R_{g_{lin}}$ are the hydrodynamic radii of the branched and linear polymer, respectively, and $[\eta]_{br}$ and $[\eta]_{lin}$ are the intrinsic viscosities of the branched and linear polymer having the same MW; for regular star-shaped polymers the exponent b is less than unity, being equal to 0.5 for the θ-solvent or to 0.6—0.8 for good solvents.[45]

In most cases the Zimm branching factor of the radius of gyration for branched polymers is less than unity. As the number of branching points increases, the parameter g decreases. Since accurate determination of the radius of gyration by light scattering is difficult, especially for polymers with low MWs, and since the intrinsic viscosity can be measured experimentally with high accuracy, it is appropriate to experimentally determine the g′ parameter rather than g. We evaluated the Zimm branching factors of intrinsic viscosity for a number of samples (see Table 6). The $[\eta]_{lin}$ values were calculated using the Mark—Kuhn—Houwink equation (4) and the absolute values of M_w determined by light scattering. From the data of Table 6 it follows that the g′ parameters of all DN-based PS samples are smaller than the corresponding g parameters of linear analogues. It should be noted that the MDN-based PS samples and the PS samples with high concentrations of BDN are characterized by the lowest g values.

The g parameters of branched macromolecules of regular structure, *viz.*, star-shaped structures with same-length arms are calculated from the expression

$$g = 3/p - 2/p^2, \quad (11)$$

where p is the number of branches.[46]

For instance, the theoretical value of the Zimm branching factor of the radius of gyration is 0.78 and 0.63 for three- and four-arm star-shaped macromolecules, respectively. Taking account of Eq. (10), the theoretical g' value in a good solvent should be approximately 0.86—0.81 for the three-arm and 0.76—0.69 for the four-arm star-shaped structures. Thus, our estimates of the g' parameters of the PS samples synthesized in the presence of DNs suggest the possibility of formation of star-shaped structures at different concentrations of MDN, PDN, and BDN (1.5 mol.%). However, it should be noted that the PS samples obtained *in situ* in the presence of DNs can be of different architecture (contain linear and branched forms, *e.g.*, three- and four-arm stars of irregular structure). In this connection, it can only be said of the apparent ρ-parameter and Zimm branching factor of intrinsic viscosity that allow one to compare different polymers and provide qualitative assessment of the effect of the number of branching points on the degree of compression of the macromolecular coil.

We also calculated the R_g^2/M_w values to evaluate the compactness,[48] one more characteristic of the behavior of macromolecules in solution, using the static light scattering data. Compactness of a macromolecular coil in solution is governed by the macromolecular conformation. The larger the R_g^2/M_w value the less compact the macromolecular coil.[48] From the data of Table 6 it follows that the compactness of macromolecular coils correlates with the ρ-parameter and the Zimm branching factor of intrinsic viscosity for all the samples studied. The most compact are the samples obtained in the presence of 0.5 mol.% MDN and PDN; compactness of the BDN-based PS increases with increasing DN concentration.

The results obtained show that DN-mediated polymerization is suitable for the synthesis of star-shaped structures. The polymers obtained in the presence of MDN and PDN are more branched than those synthesized using BDN. We believe this feature is due to instability of the HAAs formed in the presence of BDN since BDN-based nitroxides can decompose to give MNP (see Ref. 38) that mediates the formation of linear polymers. Indeed, based

on the ρ-parameter and compactness values, MDN- or PDN-mediated synthesis of polymers at a DN : AIBN ratio of 0.5 : 1 affords more branched structures than those formed at higher DN concentrations (DN : AIBN = 3 : 1). It should be noted that, theoretically, it is a DN : initiator ratio of 0.5 : 1 that is most appropriate for the formation of four-arm star-shaped structures. At a higher DN concentration, an excess amount of DN can lead to formation of linear macromolecules along with the branched structures and thus to an increase in the apparent ρ-parameter and compactness values. However, the opposite was observed in the case of BDN, *viz.*, it is the increase in the BDN concentration that allows one to synthesize branched structures. This fact is consistent with the stability of nitroxide radicals generated from BDN.

Summing up, in this work we carried out a detailed analysis of the structure and configuration of PS macromolecules obtained in the presence of α-DNs as precursors of stable nitroxide radicals. To determine the structures of HAAs, the synthesized PS samples were modified (nitroxide moiety was replaced by the cyanoisopropyl radical, bromine, and hydrogen atoms), exposed to thermolysis, and then a MALDI-TOF mass spectrometric analysis of both unmodified and modified polymers was performed. It was established that modification of the MDN- and BDN-based HAAs synthesized *in situ* during the polymerization of ST causes a considerable decrease in the MW of the samples. This is indicative of the formation of HAAs containing the nitroxide fragment within the polymer chain. In addition, it was shown that the changes in the MW of both decomposition products formed during modification of the PS samples isolated at different monomer conversions can serve an indirect proof of the formation of branched structures. Our static and dynamic light scattering study of the conformational properties of the synthesized HAAs revealed the possibility to synthesize miktoarm star-shaped polymers by varying the conditions of DN-mediated polymerization of ST irrespective of the DN structure. It was established that the key factors responsible for the formation of star-shaped structures in the presence of α-DNs include their accepting ability and the stability of the DN-based nitroxide radicals formed *in situ*, as well as the optimum concentration of glyoxaldinitrones. In particular, star-shaped macromolecules can form in the presence of excess amount of sterically hindered BDN owing to the possibility of decomposition of the corresponding nitroxide radicals. Branched macromolecules can also be obtained using lower concentrations of more thermally stable MDN and PDN.

Experimental

Reactants. Styrene (Aldrich) was purified from inhibitors by 10% aqueous NaOH, the alkali was washed off with water until neutral pH, and the solution was dried over calcined calcium chloride. Then, ST was distilled collecting the fraction with b.p. 48 °C at 20 Torr.[49] Azobisisobutyronitrile (Aldrich) was recrystallized from ethanol following a conventional procedure.[50] Dichloromethane, isopropyl alcohol, and acetone (Komponent-Reaktiv, Russia) were dried over calcined calcium chloride and distilled. Toluene (Komponent-Reaktiv, Russia) was dried over calcium chloride and then distilled over metallic sodium; DMSO was dried over sodium hydroxide and distilled at a reduced pressure. The physicochemical constants of all compounds used in this work were consistent with the published data.[51]

The nitrones MDN, BDN, and PDN were synthesized following a known procedure[52] and characterized by liquid chromatography and by IR and NMR spectroscopies.

***N,N*-Dimethylglyoxaldinitrone (MDN).** ^{1}H NMR ($CDCl_3$, 400 MHZ), δ: 3.8 (s, 6 H, CH_3); 7.8 (s, 2 H, CH=N(O)). IR (KBr), ν/cm^{-1}: 3109 (s, C—H stretching vibrations); 1547 (s, C=N stretching vibrations); 1176 (m, N—O stretching vibrations).

***N,N*-Di-*tert*-butylglyoxaldinitrone (BDN).** ^{1}H NMR ($CDCl_3$, 400 MHz), δ: 1.57 (s, 18 H, $C(CH_3)_3$); 8.27 (s, 2 H, CH=N(O)). IR (KBr), ν/cm^{-1}: 3163 (s, C—H stretching vibrations); 1504 (s, C=N stretching vibrations); 1127 (m, N—O stretching vibrations).

***N,N*-Diphenylglyoxaldinitrone (PDN).** ^{1}H NMR ($CDCl_3$, 400 MHz), δ: 7.85 (m, 4 H, *m*-C_6H_5); 7.52 (m, 6 H, *o*- and *p*-C_6H_5); 8.67 (s, 2 H, CH=N(O)). IR (KBr), ν/cm^{-1}: 3134 (s, C—H stretching vibrations); 1500 (s, C=N stretching vibrations); 1477 (m, C—C skeletal vibrations); 1092 (m, N—O stretching vibrations); 779 (m, C—H deformation vibrations).

Polymerization of ST in the presence of DN. A solution of ST (0.8 mL), a DN (0.5, 1.5, or 3 mol.%), and AIBN (1 mol.%) was placed into an ampoule. Under reduced pressure, the ampoule was three times degassed by repeating the freeze—thaw cycles until a residual pressure of $2 \cdot 10^{-2}$ Torr and sealed. The polymerization kinetics was monitored gravimetrically. After a specified time interval the ampoule was frozen in liquid nitrogen to terminate the polymerization. The polymer obtained was precipitated into isopropyl alcohol. To purify the polymers from monomer residues, the samples were reprecipitated from a dichloromethane solution and then dried until constant weight at a reduced pressure and 50°°C. The monomer conversion was calculated from the expression

$$P = m_p/m_m \cdot 100\%,$$

where m_p is the weight of the polymer and m_m is the weight of the monomer.

Modification and thermolysis of polymers. A weighed sample of a polymer (0.01 g) and a weighed sample of a modifier (CBr_4, 35Q, AIBN, $C_{12}H_{25}SH$, nitroxide N) taken in a fivefold excess (0.05 g) relative to the polymer was placed in an ampoule and a solvent (benzene, THF, and DMSO; V = 0.5 mL) was added. Modification of polymers at a reduced pressure was performed using THF and benzene. Samples were prepared as described above. Modification of polymers at atmospheric pressure in air was done in the presence of DMSO as high-boiling solvent.

The samples were kept at 90 and 110 °C for 20 h (at 130 °C, for 7 h). Then, the ampoules were opened and the products were analyzed by GPC and MALDI-TOF mass spectrometry. If the solvent was different from THF, it was replaced by THF by triple evacuation of the solvent at a reduced pressure of $2 \cdot 10^{-2}$ Torr.

Analysis of the molecular-weight characteristics of polymers. The MW characteristics of the polymers were determined by

GPC on a KNAUER liquid chromatograph equipped with a cascade of the Phenomenex columns (300 mm×7.8 mm, Phenogel, 10 μm) with pore diameters of 10^5 and 10^3 Å and two (refractometric and UV) detectors. The eluent was THF and the temperature of the column was maintained at 25.0±0.1 °C. Narrow-dispersity PS standards were used for calibration.[53]

The structures of DNs were studied on an Agilent DD2 400 spectrometer operating at 400 MHz at room temperature. The ^{1}H NMR spectra were recorded in $CDCl_3$ relative to the signal of residual protons of the deuterated solvent.

Infrared spectra of DNs were recorded on an Infralum FT-801 instrument in the wavenumber range of 5500—550 cm^{-1} with an accuracy of ±0.05 cm^{-1} using pressed KBr pellets.

Determination of the composition of the polymers by MALDI-TOF mass spectrometry. The MALDI-TOF mass spectra of the polymers were recorded on a Bruker Microflex LT instrument equipped with a nitrogen laser (λ = 337.1 nm) in the linear mode using DCTB and DHB as matrices. The spectrometer was calibrated using the (poly(methyl methacrylate), PMMA + Na)$^+$ peaks of narrow-dispersity PMMA standards (Waters, M_n = 2.58 and 8.2 kDa). The calibration curve was approximated by a cubic polynomial. Experimental data were processed using the Bruker flexControl and flexAnalysis software. Samples were prepared by mixing a solution of a polymer (5 μL, 10 mg mL^{-1}), a solution of a matrix (10 μL, 20 mg mL^{-1}), and a solution of the salt (silver trifluoroacetate, 3 μL, 5 mg mL^{-1}) in THF in a microtube. The MALDI-TOF analysis using the DHB matrix was carried out under salt-free conditions. The MALDI-TOF analysis using the DCTB matrix was performed both in the presence and in the absence of the salt. Then, the solution (2 μL) was poured onto a stainless steel support and analyzed.

Determination of the molecular-weight and hydrodynamic characteristics of polymers. The MWs and the static and hydrodynamic sizes of macromolecules were determined by static and dynamic light scattering. The hydrodynamic characteristics of the polymer macromolecules were measured on a NanoBrook Omni instrument (Brookhaven Instruments, USA). A 35-mW laser (λ_0 = 640 nm) was used as the light source. The correlation function of the scattered light intensity was obtained using a TurboCorr research-level correlator with 510 channels. The accumulation time of the correlation function was 180—300 s. The number of photons incident on the detector was in the range of 50—450 per second. The average hydrodynamic diameter was calculated from the values obtained in 5—10 parallel measurements. Prior to the experiments, a quartz cell was dedusted by rinsing two or three times with a solvent filtered through a Chromafil™ Xtra Nylon filter with a pore diameter of 0.2 μm. The measurements were carried out at a scattering angle, θ, of 173°. The hydrodynamic radii (R_h) were determined using the Stokes—Einstein equation. The solvent was toluene (density ρ = 0.862 g cm^{-3}, the dynamic viscosity η_0 = 0.560 cP, and the refractive index n_0 = 1.494). All experiments were carried out at 25°°C. The test solutions were filtered through Chromafil™ Xtra Nylon filters with a pore diameter of 0.2 μm.

The M_w values and the radius of gyration (R_g) were determined by the Debye method[54] and by the Zimm double extrapolation method using the data of static light scattering measurements on a BI-MwA molecular Weight Analyzer (Brookhaven Instruments, USA). A 30-mW laser (λ_0 = 660 nm) with vertical polarization was used as the light source.

The refractive index increment was measured on a BI-DNDC differential refractometer (Brookhaven Instruments, USA). The derivative, dn/dc, was determined from the slope of the dependence of the refractive index of the test solution on the polymer concentration. The intrinsic viscosity [η] of the polymers was measured in toluene using Ostwald capillary viscometers (solvent flow time t_0 = 49.4 s) at 25 °C.

The authors express their gratitude to I. D. Grishin for carrying out MALDI-TOF mass spectrometric analysis.

This work was financially supported by the Russian Foundation for Basic Research (Project No. 20-03-00150).

This paper does not contain descriptions of studies on animals or humans.

The authors declare no competing interests.

References

1. D. F. Grishin, I. D. Grishin, *Russ. Chem. Rev.* (*Engl. Transl.*), 2021, **90**, 231; DOI: 10.1070/RCR4964.
2. N. Corrigan, K. Jung, G. Moad, C. J. Hawker, K. Matyjaszewski, C. Boyer, *Prog. Polym. Sci.*, 2020, **111**, 101311; DOI: 10.1016/j.progpolymsci.2020.101311.
3. *Reversible Deactivation Radical Polymerization: Mechanisms and Synthetic Methodologies*, Ed. K. Matyjaszewski, H. Gao, B. S. Sumerlin, N. V. Tsarevsky, American Chemical Society, Washington, 2018, 480 p.
4. O. S. Lizyakina, L. B. Vaganova, A. V. Piskunov, D. F. Grishin, *Russ. Chem. Bull.,* 2020, **69**, 1478; DOI: 10.1007/s11172-020-2926-0.
5. D. F. Grishin, I. D. Grishin, in *Polymeric Materials for Clean Water*, Ed. R. Das, Springer, Switzerland, 2019, 7.
6. A. Anastasaki, J. Willenbacher, C. Fleischmann, W. R. Gutekunst, C. J. Hawker, *Polym. Chem.*, 2017, **8**, 689; DOI: 10.1039/C6PY01993E.
7. A. I. Amirova, T. U. Kirila, A. N. Blokhin, A. B. Razina, A. E. Bursian, A. V. Tenkovtsev, A. P. Filippov, *Mendeleev Commun.*, 2020, **30**, 502; DOI: 10.1016/j.mencom.2020.07.033.
8. P. A. Tikhonov, N. G. Vasilenko, G. V. Cherkaev, V. G. Vasil´ev, N. V. Demchenko, E. A. Tatarinova, A. M. Muzafarova, *Mendeleev Commun.*, 2019, **29**, 625; DOI: 10.1016/j.mencom.2019.11.006.
9. *Nitroxide Mediated Polymerization from Fundamentals to Applications in Materials Science*, Ed. D. Gigmes, The Royal Society of Chemistry, UK, 2016, 500 p.
10. J. Nicolas, Y. Guillaneuf, C. Lefay, D. Bertin, D. Gigmes, B. Charleux, *Prog. Polym. Sci.*, 2013, **38**, 63; DOI: 10.1016/j.progpolymsci.2012.06.002.
11. M. Edeleva, G. Audran, S. Marque, E. Bagryanskaya, *Materials*, 2019, **12**, 688; DOI: 10.3390/ma12050688.
12. V. Sciannamea, R. Jérôme, C. Detrembleur, *Chem. Rev.*, 2008, **108**, 1104; DOI: 10.1021/cr0680540.
13. E. V. Kolyakina, D. F. Grishin, *Russ. Chem. Rev.*, 2009, **78**, 535; DOI: 10.1070/RC2009v078n06ABEH004026.
14. D. F. Grishin, L. L. Semenycheva, E. V. Kolyakina, *Dokl. AN*, 1998, **362**, 634 [*Dokl. Chem.* (*Engl. Transl.*), 1998, **362**, 634].
15. E. V. Kolyakina, L. L. Semenycheva, D. F. Grishin, *Vysokomolekulyar. soedineniya*, *Ser. A*, 2001, **43**, 2092 [*Polym. Sci.*, *Ser. A.* (*Engl. Transl.*), 2001, **43**, 1223].
16. M. Yu. Zaremski, A. P. Orlova, E. S. Garina, A. V. Olenin, M. B. Lachinov, V. B. Golubev, *Vysokomolekulyar. soedineniya*,

Ser. A, 2003, **45**, 871 [*Polym. Sci*., *Ser. A* (*Engl. Transl.*), 2003, **45**, 502].
17. M. Yu. Zaremski, A. L. Reznichenko, Yu. V. Grinevich, E. S. Garina, M. B. Lachinov, V. B. Golubev, *Vysokomolekulyar. soedineniya*, *Ser. A*, 2005, **47**, 898 [*Polym. Sci*., *Ser. A* (*Engl. Transl.*), 2005, **47**, 536].
18. E. V. Kolyakina, A. B. Alyeva, D. F. Grishin*, Applied Solid State Chemistry*, 2018, **2**, 29.
19. E. V. Kolyakina, A. B. Alyeva, E. V. Sazonova, A. A. Shchepalov, D. F. Grishin, *Russ. Chem. Bull.,* 2019, **68**, 1585; DOI: 10.1007/s11172-019-2597-x.
20. E. V. Kolyakina, A. B. Alyeva, E. V. Sazonova, E. A. Zakharychev, D. F. Grishin, *Vysokomolekulyar. soedineniya*, *Ser. B*, 2020, **62**, 253; DOI: 10.31857/S2308113920040075 [*Polym. Sci*., *Ser. B* (*Engl. Transl.*), **62**, 328 DOI: 10.1134/S1560090420040077].
21. V. Sciannamea, C. Guerrero-Sanchez, U. S. Schuert, J. M. Catala, R. Jerome, C. Detrembleur, *Polymer*, 2005, **46**, 9632; DOI: 10.1016/j.polymer.2005.07.074.
22. V. Sciannamea*,* J. M. Catala, R. Jerome, C. Detrembleur, *J. Polym. Sci*., *Part A: Polym. Chem*., 2007, **45**, 1219; DOI: 10.1002/pola.21889.
23. E. H. H. Wong, T. Junkers, C. Barner-Kowollik, *J. Polym. Sci.*, *Part A: Polym. Chem.*, 2008, **46**, 7273; DOI: 10.1002/pola.23025.
24. T. Junkers, E. H. H. Wong, M. H. Stenzel, C. Barner-Kowollik, *Macromolecules*, 2009, **42**, 5027; DOI: 10.1021/ma900356p.
25. L. Barner, A. S. Quick, A. P. Vogt, V. Winkler, T. Junkers, C. Barner-Kowollik, *Polym. Chem.*, 2012, **3**, 2266; DOI: 10.1039/C2PY20272G.
26. G. Wang, J. Huang, *Polym. Chem.*, 2014, **5**, 277; DOI: 10.1039/C3PY00872J.
27. E. H. H. Wong, O. Altintas, M. H. Stenzel, C. Barner-Kowollik, T. Junkers, *Chem. Commun.*, 2011, **47**, 5491; DOI: 10.1039/C1CC10322A.
28. S. C. Radzinski, E. S. Tillman, *Polymer*, 2011, **52**, 6003; DOI: 10.1016/j.polymer.2011.10.053
29. K. Xia, A. J. Rubaie, B. P. Johnson, S. A. Parker, E. S. Tillman, *J. Polym. Sci*., *Part A: Polym. Chem.*, 2019, **57**, 2113; DOI: 10.1002/pola.29482.
30. C. Detrembleur, A. Debuigne, O. Altintas, M. Conradi, E. H. H. Wong, C. Jerome, C. Barner-Kowollik, T. Junkers, *Polym. Chem.*, 2012, **3**, 135; DOI: 10.1039/C1PY00297J.
31. C. S. Blackburn, K. D. Myers, E. S. Tillman, *Polymer*, 2015, **68**, 284; DOI: 10.1016/j.polymer.2015.05.021.
32. B. D. McFadden, M. M. Arce, E. M. Carnicom, J. Herman, J. Abruzzese, E. S. Tillman, *Macromol. Chem. Phys*., 2016, **217**, 2473; DOI: 10.1002/macp.201600317.
33. M. Du, C. Deng, X. Wu, H. Liu, H. Liu, *Macromol. Chem. Phys*., 2017, **218**, DOI: 10.1002/macp.201700069.
34. E. V. Kolyakina, F. Kh. Shoipova, A. B. Alyeva, D. F. Grishin, *Russ. Chem. Bull.,* 2021, **70**, 1736.
35. E. H. H. Wong, T. Junkers, C. Barner-Kowollik, *Polym. Chem*., 2011, **2**, 1008; DOI: 10.1039/C0PY00377H.
36. A. B. Cook, S. Perrier, *Adv. Funct. Mater.*, 2020, **30**, 1901001; DOI: 10.1002/adfm.201901001.
37. W. Wua, W. Wanga, J. Li, *Progress in Polymer Science*, 2015, **46**, 55; DOI: 10.1016/j.progpolymsci.2015.02.002.
38. D. Rehorek, E. G. Janzen, *J. Praktische Chemie*, 1985, **327**, 968; DOI: 10.1002/prac.19853270615.
39. V. Lotocki, K. Ashok, *Pharmaceutics*, 2020, **12**, 827; DOI: 10.3390/pharmaceutics12090827.
40. N. Fuhrman, R. B. Mesrobian, *J. Am. Chem. Soc*., 1954, **76**, 3281; DOI: 10.1021/ja01641a061.
41. F. R. Mayo, *J. Am. Chem. Soc.*, 1968, **90**, 1289. DOI: 10.1021/ja01007a032.
42. P. Outer, C. I. Carr, B. H. Zimm, *J. Chem. Phys.*, 1950. **18**, 830; DOI: 10.1063/1.1747783.
43. A. P. Filippov, O. G. Zamyshlyayeva, E. B. Tarabukina, M. A. Simonova, A. V. Kozlov, Yu. D. Semchikov, *Vysokomolekulyar. soedineniya*, *Ser. A*, **54,** 675 [*Polym. Sci*., *Ser. A* (*Engl. Transl.*), 2012, **54**; DOI: 10.1134/S0965545X12050033].
44. W. Burchard, *Adv. Polymer Sci.*, 2005, **143**, 113; DOI: 10.1007/b136243.
45. W. Huang, W. Gu, H. Yang, X. Xue, B. Jiang, D. Zhang, J. Fang, J. Chen, Y. Yang, J. Guo, *Polymers*, 2017, **9**, DOI: 10.3390/polym9010014.
46. T. A. Orofino, *Polymer*, 1961, **2**, 305; DOI: 10.1016/0032-3861(61)90033-7.
47. P. G. de Gennes, *Macromol.*, 1980, **13**, 1069; DOI: 10.1021/ma60077a009.
48. N. V. Kutsevol, T. N. Bezuglaya, M. Y. Bezuglyi, *Russ. J. Struct. Chem.*, 2014, **55**, 548; DOI: 10.1134/S002247661403024X.
49. *Entsiklopediya polimerov* [*Polymer Encyclopedia*], Ed. V. A. Kabanov, Moscow, Sovetskaya Entsiklopediya, 1972, vol. **1** (in Russian).
50. Organic Syntheses, New York—London, Interscience Publishers, 1946—1952, V. **26—32**.
51. A. Weissberger, E. Proskauer, J. Riddick, E. Toops, *Organic Solvents*, Interscience Publishers, New York, 1955.
52. I. Raspertova, O. Osetska, K. Gubina, R. Lampeka, *Polyhedron*, 2011, **30**, 2320; DOI: 10.1016/j.poly.2011.06.015.
53. B. G. Belen′kiy, L. Z. Vilenchik, *Khromatografiya polimerov* [*Chromatography of Polymers*], Khimiya, Moscow, 1978, 344 pp. (in Russian).
54. V. E. Eskin, *Rasseyanie sveta rastvorami polimerov* [*Light Scattering by Solutions of Polymers*], Nauka, Leningrad, 1986, 286 pp. (in Russian).

Received March 29, 2021;
in revised form June 21, 2021;
accepted July 6, 2021